

# Synchronised firing patterns in a random network of adaptive exponential integrate-and-fire

F. S. Borges<sup>1</sup>, P. R. Protachevich<sup>1</sup>, E. L. Lameu<sup>1</sup>, R. C. Bonetti<sup>1</sup>, K. C. Iarosz<sup>2</sup>, I. L. Caldas<sup>2</sup>, M. S. Baptista<sup>3</sup>, A. M. Batista<sup>1,2,4,\*</sup>

<sup>1</sup>*Pós-Graduação em Ciências/Física, Universidade Estadual de Ponta Grossa, Ponta Grossa, PR, Brazil.*

<sup>2</sup>*Instituto de Física, Universidade de São Paulo, São Paulo, SP, Brazil.*

<sup>3</sup>*Institute for Complex Systems and Mathematical Biology, Aberdeen, SUPA, UK.*

<sup>4</sup>*Departamento de Matemática e Estatística, Universidade Estadual de Ponta Grossa, Ponta Grossa, PR, Brazil.*

---

## Abstract

We have studied neuronal synchronisation in a random network of adaptive exponential integrate-and-fire neurons. We study how spiking or bursting synchronous behaviour appears as a function of the coupling strength and the probability of connections, by constructing parameter spaces that identify these synchronous behaviours from measurements of the inter-spike interval and the calculation of the order parameter. Moreover, we verify the robustness of synchronisation by applying an external perturbation to each neuron. The simulations show that bursting synchronisation is more robust than spike synchronisation.

*Keywords:* synchronisation, integrate-and-fire, network

---

## 1. Introduction

The concept of synchronisation is based on the adjustment of rhythms of oscillating systems due to their interaction [1]. Synchronisation phenomenon was recognised by Huygens in the 17th century, time when he performed experiments to understand this phenomenon [2]. To date, several kinds of

---

\*Corresponding author: antoniomarcosbatista@gmail.com

synchronisation among coupled systems were reported, such as complete [3], phase [4, 5], lag [6], and collective almost synchronisation [7].

Neuronal synchronous rhythms have been observed in a wide range of researches about cognitive functions [8, 9]. Electroencephalography and magnetoencephalography studies have been suggested that neuronal synchronization in the gamma frequency plays a functional role for memories in humans [10, 11]. Steinmetz et al. [12] investigated the synchronous behaviour of pairs of neurons in the secondary somatosensory cortex of monkey. They found that attention modulates oscillatory neuronal synchronisation in the somatosensory cortex. Moreover, in the literature it has been proposed that there is a relationship between conscious perception and synchronisation of neuronal activity [13].

We study spiking and bursting synchronisation between neuron in a neuronal network model. A spike refers to the action potential generated by a neuron that rapidly rises and falls [14], while bursting refers to a sequence of spikes that are followed by a quiescent time [15]. It was demonstrated that spiking synchronisation is relevant to olfactory bulb [16] and is involved in motor cortical functions [17]. The characteristics and mechanisms of bursting synchronisation were studied in cultured cortical neurons by means of planar electrode array [18]. Jefferys & Haas discovered synchronised bursting of CA1 hippocampal pyramidal cells [19].

There is a wide range of mathematical models used to describe neuronal activity, such as the cellular automaton [20], the Rulkov map [21], and differential equations [22, 23]. One of the simplest mathematical models and that is widely used to depict neuronal behaviour is the integrate-and-fire [24], which is governed by a linear differential equation. A more realistic version of it is the adaptive exponential integrate-and-fire (aEIF) model which we consider in this work as the local neuronal activity of neurons in the network. The aEIF is a two-dimensional integrate-and-fire model introduced by Brette & Gerstner [25]. This model has an exponential spike mechanism with an adaptation current. Touboul & Brette [26] studied the bifurcation diagram of the aEIF. They showed the existence of the Andronov-Hopf bifurcation and saddle-node bifurcations. The aEIF model can generate multiple firing patterns depending on the parameter and which fit experimental data from cortical neurons under current stimulation [27].

In this work, we focus on the synchronisation phenomenon in a randomly connected network. This kind of network, also called Erdős-Rényi network [28], has nodes where each pair is connected according to a prob-

ability. The random neuronal network was utilised to study oscillations in cortico-thalamic circuits [29] and dynamics of network with synaptic depression [30]. We built a random neuronal network with unidirectional connections that represent chemical synapses.

We show that there are clearly separated ranges of parameters that lead to spiking or bursting synchronisation. In addition, we analyse the robustness to external perturbation of the synchronisation. We verify that bursting synchronisation is more robustness than spiking synchronisation. However, bursting synchronisation requires larger chemical synaptic strengths, and larger voltage potential relaxation reset to appear than those required for spiking synchronisation.

This paper is organised as follows: in Section II we present the adaptive exponential integrate-and-fire model. In Section III, we introduce the neuronal network with random features. In Section IV, we analyse the behaviour of spiking and bursting synchronisation. In the last Section, we draw our conclusions.

## 2. Adaptive exponential integrate-and-fire

As a local dynamics of the neuronal network, we consider the adaptive exponential integrate-and-fire (aEIF) model that consists of a system of two differential equations [25] given by

$$\begin{aligned} C \frac{dV}{dt} &= -g_L(V - E_L) + \Delta_T \exp\left(\frac{V - V_T}{\Delta_T}\right) \\ &\quad + I - w, \\ \tau_w \frac{dw}{dt} &= a(V - E_L) - w, \end{aligned} \tag{1}$$

where  $V(t)$  is the membrane potential when a current  $I(t)$  is injected,  $C$  is the membrane capacitance,  $g_L$  is the leak conductance,  $E_L$  is the resting potential,  $\Delta_T$  is the slope factor,  $V_T$  is the threshold potential,  $w$  is an adaptation variable,  $\tau_w$  is the time constant, and  $a$  is the level of subthreshold adaptation. If  $V(t)$  reaches the threshold  $V_{\text{peak}}$ , a reset condition is applied:  $V \rightarrow V_r$  and  $w \rightarrow w_r = w + b$ . In our simulations, we consider  $C = 200.0\text{pF}$ ,  $g_L = 12.0\text{nS}$ ,  $E_L = -70.0\text{mV}$ ,  $\Delta_T = 2.0\text{mV}$ ,  $V_T = -50.0\text{mV}$ ,  $I = 509.7\text{pA}$ ,  $\tau_w = 300.0\text{ms}$ ,  $a = 2.0\text{nS}$ , and  $V_{\text{peak}} = 20.0\text{mV}$  [27].

The firing pattern depends on the reset parameters  $V_r$  and  $b$ . Table 1 exhibits some values that generate five different firing patterns (Fig. 1).

In Fig. 1 we represent each firing pattern with a different colour in the parameter space  $b \times V_r$ : adaptation in red, tonic spiking in blue, initial bursting in green, regular bursting in yellow, and irregular in black. In Figs. 1a, 1b, and 1c we observe adaptation, tonic spiking, and initial burst pattern, respectively, due to a step current stimulation. Adaptation pattern has increasing inter-spike interval during a sustained stimulus, tonic spiking pattern is the simplest regular discharge of the action potential, and the initial bursting pattern starts with a group of spikes presenting a frequency larger than the steady state frequency. The membrane potential evolution with regular bursting is showed in Fig. 1d, while Fig. 1e displays irregular pattern.

Table 1: Reset parameters.

Firing patterns	Fig.	b (pA)	$V_r$ (mV)	Layout
adaptation	1(a)	60.0	-68.0	red
tonic spiking	1(b)	5.0	-65.0	blue
initial burst	1(c)	35.0	-48.8	green
regular bursting	1(d)	40.0	-45.0	yellow
irregular	1(e)	41.2	-47.4	black

As we have interest in spiking and bursting synchronisation, we separate the parameter space into a region with spike and another with bursting patterns (Fig. 2). To identify these two regions of interest, we use the coefficient of variation (CV) of the neuronal inter-spike interval (ISI), that is given by

$$CV = \frac{\sigma_{ISI}}{\bar{ISI}}, \quad (2)$$

where  $\sigma_{ISI}$  is the standard deviation of the ISI normalised by the mean  $\bar{ISI}$  [31]. Spiking patterns produce  $CV < 0.5$ . Parameter regions that represent the neurons firing with spiking pattern are denoted by gray colour in Fig. 2. Whereas, the black region represents the bursting patterns, which results in  $CV \geq 0.5$ .

### 3. Spiking or bursting synchronisation

In this work, we constructed a network where the neurons are randomly connected [28]. Our network is given by

$$C \frac{dV_i}{dt} = -g_L(V_i - E_L) + \Delta_T \exp\left(\frac{V_i - V_T}{\Delta_T}\right)$$

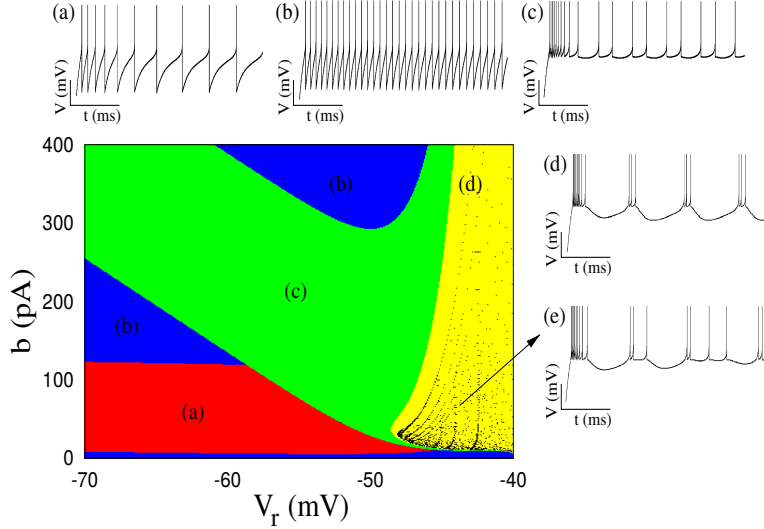


Figure 1: (Colour online) Parameter space for the firing patterns as a function of the reset parameters  $V_r$  and  $b$ . (a) Adaptation in red, (b) tonic spiking in blue, (c) initial bursting in green, (d) regular bursting in yellow, and (e) irregular in black.

$$\begin{aligned}
 & + I_i - w_i + g_{\text{ex}}(V_{\text{ex}} - V_i) \sum_{j=1}^N A_{ij} s_j + \Gamma_i, \\
 \tau_w \frac{dw_i}{dt} & = a_i(V_i - E_L) - w_i, \\
 \tau_{\text{ex}} \frac{ds_i}{dt} & = -s_i.
 \end{aligned} \tag{3}$$

where  $V_i$  is the membrane potential of the neuron  $i$ ,  $g_{\text{ex}}$  is the synaptic conductance,  $V_{\text{ex}}$  is the synaptic reversal potential,  $\tau_{\text{ex}}$  is the synaptic time constant,  $s_i$  is the synaptic weight,  $A_{ij}$  is the adjacency matrix,  $\Gamma_i$  is the external perturbation, and  $a_i$  is randomly distributed in the interval  $[1.9, 2.1]$ .

The schematic representation of the neuronal network that we have considered is illustrated in Fig 3. Each neuron is randomly linked to other neurons with a probability  $p$  by means of directed connections. When  $p$  is equal to 1, the neuronal network becomes an all-to-all network. A network with this topology was used by Borges et al. [32] to study the effects of the spike timing-dependent plasticity on the synchronisation in a Hodgkin-Huxley neuronal network.

A useful diagnostic tool to determine synchronous behaviour is the com-

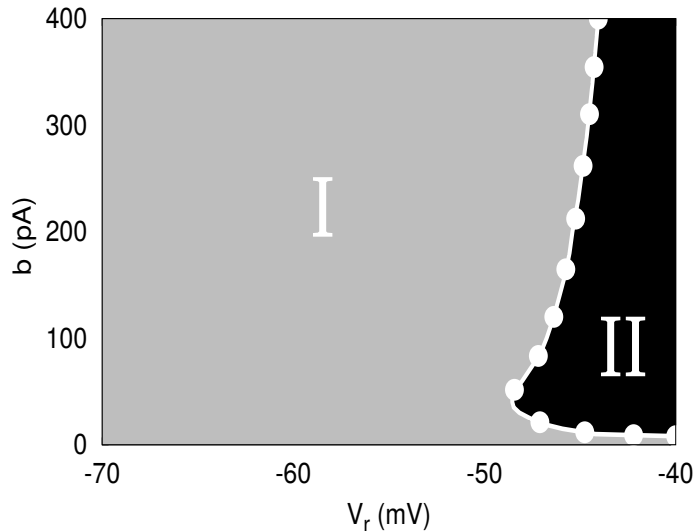


Figure 2: Parameter space for the firing patterns as a function of the reset parameters  $V_r$  and  $b$ . Spike pattern in region I ( $CV < 0.5$ ) and bursting pattern in region II ( $CV \geq 0.5$ ) are separated by white circles.

plex phase order parameter defined as [33]

$$z(t) = R(t) \exp(i\Phi(t)) \equiv \frac{1}{N} \sum_{j=1}^N \exp(i\psi_j), \quad (4)$$

where  $R$  and  $\Phi$  are the amplitude and angle of a centroid phase vector, respectively, and the phase is given by

$$\psi_j(t) = 2\pi m + 2\pi \frac{t - t_{j,m}}{t_{j,m+1} - t_{j,m}}, \quad (5)$$

where  $t_{j,m}$  corresponds to the time when a spike  $m$  ( $m = 0, 1, 2, \dots$ ) of a neuron  $j$  happens ( $t_{j,m} < t < t_{j,m+1}$ ). We have considered the beginning of the spike when  $V_j > -20$ mV. The value of the order parameter magnitude goes to 1 in a totally synchronised state. To study the neuronal synchronisation of the network, we have calculated the time-average order-parameter, that is given by

$$\bar{R} = \frac{1}{t_{\text{fin}} - t_{\text{ini}}} \sum_{t_{\text{ini}}}^{t_{\text{fin}}} R(t), \quad (6)$$

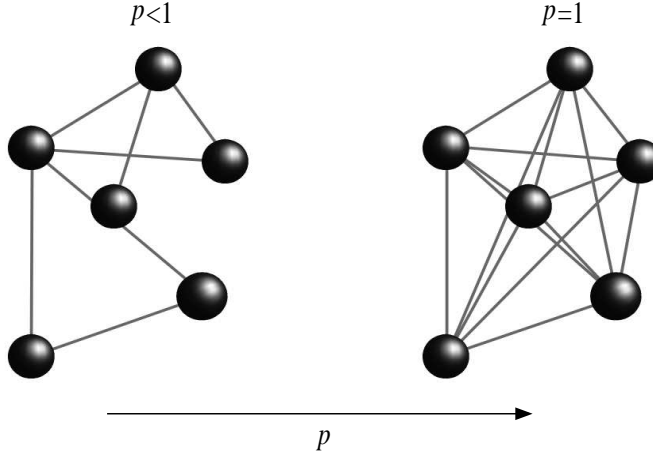


Figure 3: Schematic representation of the neuronal network where the neurons are connected according to a probability  $p$ .

where  $t_{\text{fin}} - t_{\text{ini}}$  is the time window for calculating  $\bar{R}$ .

Figs. 4a, 4b, and 4c show the raster plots for  $g_{\text{ex}} = 0.02\text{nS}$ ,  $g_{\text{ex}} = 0.19\text{nS}$ , and  $g_{\text{ex}} = 0.45\text{nS}$ , respectively, considering  $V_r = -58\text{mV}$ ,  $p = 0.5$ , and  $b = 70\text{pA}$ , where the dots correspond to the spiking activities generated by neurons. For  $g_{\text{ex}} = 0.02\text{nS}$  (Fig. 4a) the network displays a desynchronised state, and as a result, the order parameter values are very small (black line in Fig. 4d). Increasing the synaptic conductance for  $g_{\text{ex}} = 0.19\text{nS}$ , the neuronal network exhibits spike synchronisation (Fig. 4b) and the order parameter values are near unity (red line in Fig. 4d). When the network presents bursting synchronisation (Fig. 4c), the order parameter values vary between  $R \approx 1$  and  $R \ll 1$  (blue line in Fig. 4d).  $R \ll 1$  to the time when the neuron are firing.

In Fig. 5a we show  $\bar{R}$  as a function of  $g_{\text{ex}}$  for  $p = 0.5$ ,  $b = 50\text{pA}$  (black line),  $b = 60\text{pA}$  (red line), and  $b = 70\text{pA}$  (blue line). The three results exhibit strong synchronous behaviour ( $\bar{R} > 0.9$ ) for many values of  $g_{\text{ex}}$  when  $g_{\text{ex}} \gtrsim 0.4\text{nS}$ . However, for  $g_{\text{ex}} \lesssim 0.4\text{nS}$ , it is possible to see synchronous behaviour only for  $b = 70\text{pA}$  in the range  $0.15\text{nS} < g_{\text{ex}} < 0.25\text{nS}$ . In addition, we calculate the coefficient of variation (CV) to determine the range in  $g_{\text{ex}}$  where the neurons of the network have spiking or bursting behaviour (Fig. 5b). We consider that for  $\text{CV} < 0.5$  (black dashed line) the neurons exhibit spiking behaviour, while for  $\text{CV} \geq 0.5$  the neurons present bursting behaviour. We observe that in the range  $0.15\text{nS} < g_{\text{ex}} < 0.25\text{nS}$  for  $b = 70\text{pA}$  there is

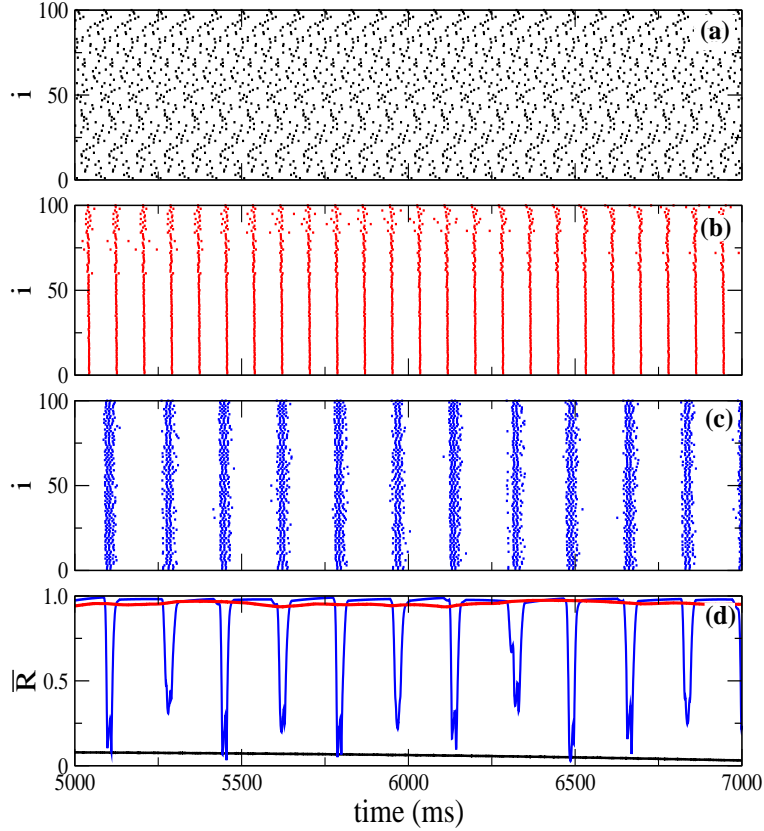


Figure 4: (Colour online) Raster plot for (a)  $g_{\text{ex}} = 0.02\text{nS}$ , (b)  $g_{\text{ex}} = 0.19\text{nS}$ , and (c)  $g_{\text{ex}} = 0.45\text{nS}$ , considering  $V_r = -58\text{mV}$ ,  $p = 0.5$ , and  $b = 70\text{pA}$ . In (d) the order parameter is computed for  $g_{\text{ex}} = 0.02\text{nS}$  (black line),  $g_{\text{ex}} = 0.19\text{nS}$  (red line), and  $g_{\text{ex}} = 0.45\text{nS}$  (blue line).

spiking synchronisation, and bursting synchronisation for  $g_{\text{ex}} \gtrsim 0.4\text{nS}$ .

#### 4. Parameter space of synchronisation

The synchronous behaviour depends on the synaptic conductance and the probability of connections. Fig. 6 exhibits the time-averaged order parameter in colour scale as a function of  $g_{\text{ex}}$  and  $p$ . We verify a large parameter region where spiking and bursting synchronisation is strong, characterised by  $\bar{R} > 0.9$ . The regions I and II correspond to spiking and bursting patterns, respectively, and these regions are separated by a white line with circles. We obtain the regions by means of the coefficient of variation (CV). There is a



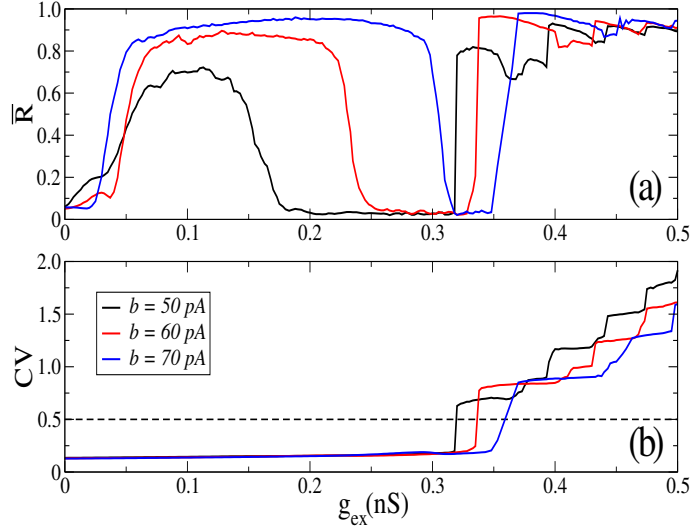


Figure 5: (Colour online) (a) Time-average order parameter and (b) CV for  $V_r = -58$ mV,  $p = 0.5$ ,  $b = 50$ pA (black line),  $b = 60$ pA (red line), and  $b = 70$ pA (blue line).

transition between region I and region II, where neurons initially synchronous in the spike, loose spiking synchronicity to give place to a neuronal network with a regime of bursting synchronisation.

We investigate the dependence of spiking and bursting synchronisation on the control parameters  $b$  and  $V_r$ . To do that, we use the time average order parameter and the coefficient of variation. Figure 7 shows that the spike patterns region (region I) decreases when  $g_{ex}$  increases. This way, the region I for  $b < 100$ pA and  $V_r = -49$ mV of parameters leading to no synchronous behaviour (Fig. 7a), becomes a region of parameters that promote synchronised bursting (Fig. 7b and 7c). However, a large region of desynchronised bursting appears for  $g_{ex} = 0.25$ nS about  $V_r = -45$ mV and  $b > 100$ pA in the region II (Fig. 7b). For  $g_{ex} = 0.5$ nS, we see, in Fig. 7c, three regions of desynchronous behaviour, one in the region I for  $b < 100$ pA, other in region II for  $b < 200$ pA, and another one is located around the border (white line with circles) between regions I and II for  $b > 200$ pA.

It has been found that external perturbations on neuronal networks not only can induce synchronous behaviour [34, 35], but also can suppress synchronisation [36]. Aiming to study the robustness to perturbations of the synchronous behaviour, we consider an external perturbation  $\Gamma_i$  (3). It is applied on each neuron  $i$  with an average time interval of about 10ms and

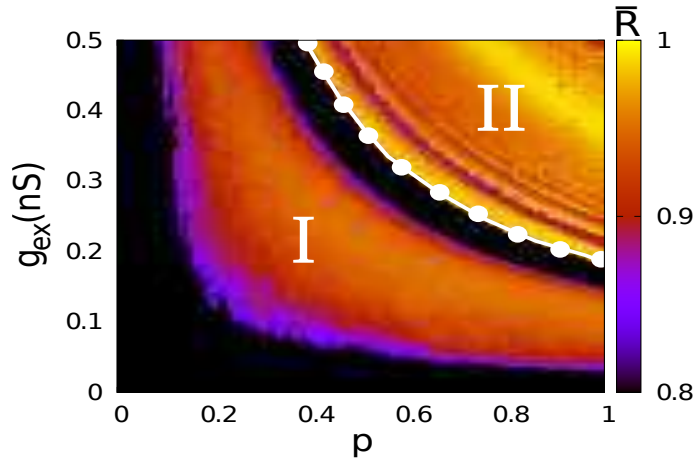


Figure 6: (Colour online)  $g_{\text{ex}} \times p$  for  $V_r = -58\text{mV}$  and  $b = 70\text{pA}$ , where the colour bar represents the time-average order parameter. The regions I (spike patterns) and II (bursting patterns) are separated by the white line with circles.

with a constant intensity  $\gamma$  during 1ms.

Figure 8 shows the plots  $g_{\text{ex}} \times p$  for  $\gamma > 0$ , where the regions I and II correspond to spiking and bursting patterns, respectively, separated by white line with circles, and the colour bar indicates the time-average order parameter values. In this Figure, we consider  $V_r = -58\text{mV}$ ,  $b = 70\text{pA}$ , (a)  $\gamma = 250\text{pA}$ , (b)  $\gamma = 500\text{pA}$ , and (c)  $\gamma = 1000\text{pA}$ . For  $\gamma = 250\text{pA}$  (Fig. 8a) the perturbation does not suppress spike synchronisation, whereas for  $\gamma = 500\text{pA}$  the synchronisation is completely suppressed in region I (Fig. 8b). In Fig. 8c, we see that increasing further the constant intensity for  $\gamma = 1000\text{pA}$ , the external perturbation suppresses also bursting synchronisation in region II. Therefore, the synchronous behavior in region II is more robustness to perturbations than in the region I, due to the fact that the region II is in a range with high  $g_{\text{ex}}$  and  $p$  values, namely strong coupling and high connectivity.

In order to understand the perturbation effect on the spike and bursting patterns, we consider the same values of  $g_{\text{ex}}$  and  $p$  as Fig. 7a. Figure 9 exhibits the space parameter  $b \times V_r$ , where  $\gamma$  is equal to  $500\text{pA}$ . The external perturbation suppresses synchronisation in the region I, whereas we observe synchronisation in region II. The synchronous behaviour in region II can be suppressed if the constant intensity  $\gamma$  is increased. Therefore, bursting synchronisation is more robustness to perturbations than spike synchronisation.

## 5. Conclusion

In this paper, we studied the spiking and bursting synchronous behaviour in a random neuronal network where the local dynamics of the neurons is given by the adaptive exponential integrate-and-fire (aEIF) model. The aEIF model can exhibit different firing patterns, such as adaptation, tonic spiking, initial burst, regular bursting, and irregular bursting.

In our network, the neurons are randomly connected according to a probability. The larger the probability of connection, and the strength of the synaptic connection, the more likely is to find bursting synchronisation.

It is possible to suppress synchronous behaviour by means of an external perturbation. However, synchronous behaviour with higher values of  $g_{\text{ex}}$  and  $p$ , which typically promotes bursting synchronisation, are more robust to perturbations, then spike synchronous behaviour appearing for smaller values of these parameters. We concluded that bursting synchronisation provides a good environment to transmit information when neurons are strongly perturbed (large  $\Gamma$ ).

## Acknowledgements

This study was possible by partial financial support from the following Brazilian government agencies: CNPq, CAPES, and FAPESP (2011/19296-1 and 2015/07311-7). We also wish thank Newton Fund and COFAP.

## References

- [1] Pikovsky, A., Rosenblum, M., Kurths, J. (2001). Synchronization: A universal concept in nonlinear sciences. Cambridge University Press.
- [2] Bennet, M., Schatz, M. F., Rockwood, H., Wiesenfeld, K. (2002). Huygens's clocks. *Proceedings: Mathematical, Physical and Engineering Sciences*, 458, 563-579.
- [3] Li, Y. & Li, C. (2016). Complete synchronization of delayed chaotic neural networks by intermittent control with two switches in a control period. *Neurocomputing*, 173, 1341-1347.
- [4] Pereira, T., Baptista, M. S., Kurths, J. (2007). Onset of phase synchronisation in neurons with chemical synapse. *International Journal of Bifurcation and Chaos*, 17, 3545-3549.

- [5] Batista, C. A. S., Lopes, S. R., Viana, R. L., Batista, A. M. (2010). Delayed feedback control of bursting synchronization in a scale-free neuronal network. *Neural Networks*, 23, 114-124.
- [6] Huang, J., Li, C., Huang, T., He, X. (2014). Finite-time lag synchronization of delayed neural networks. *Neurocomputing*, 139, 145-149.
- [7] Baptista, M. S., Ren, H.-P., Swarts, J. C. M., Carareto, R., Nijmeijer, H., Grebogi, C. (2012). Collective Almost Synchronisation in Complex Networks. *Plos One*, 7, e48118.
- [8] Wang, X.-J. (2010). Neurophysiological and Computational Principles of Cortical Rhythms in Cognition. *Physiological Reviews*, 90, 1195-1268.
- [9] Hutcheon, B., Yarom, Y. (2000). Resonance oscillation and the intrinsic frequency preferences of neurons. *Trends In NeuroScience*, 23, 216-222.
- [10] Axmacher, N., Mormann, F., Fernandez, G., Elger, C. E., Fell, J. (2006). Memory formation by neuronal synchronization. *Brain Research Reviews*, 52, 170-182.
- [11] Fell, J. & Axmacher, N. (2011). The role of phase synchronization in memory processes. *Nature Reviews Neuroscience*, 12, 105-118.
- [12] Steinmetz, P. N., Roy, A., Fitzgerald, P. J., Hsiao, S. S., Johnson, K. O., Niebur, E. (2000). Attention modulates synchronized neuronal firing in primate somatosensory cortex. *Nature*, 404, 187-190.
- [13] Hipp, J. F., Engel, A. K., Siegel, M. (2011). Oscillatory synchronization in large-scale cortical networks predicts perception. *Neuron*, 69, 387-396.
- [14] de Lange, E. & Hasler, M. (2008). Predicting single spikes and spike patterns with the Hindmarsh-Rose model. *Biological Cybernetics*, 99, 349-360.
- [15] Wu, Y., Lu, W., Lin, W., Leng, G., Feng, J. (2012). Bifurcations of emergent bursting in a neuronal network. *Plos One*, 7, e38402.
- [16] Davison, A. P., Feng, J., Brown, D. (2001). Spike synchronization in a biophysically-detailed model of the olfactory bulb. *Neurocomputing*, 38, 515-521.

- [17] Riehle, A., Grun, S., Diesmann, M., Aertsen, A. (1997). Spike synchronization and rate modulation differentially involved in motor cortical function. *Science*, 278, 1950-1953.
- [18] Maeda, E., Robinson P. C., Kawana A. (1995). The mechanisms of generation and propagation of synchronized bursting in developing networks of cortical neurons. *The Journal of Neuroscience*, 15, 6834-6845.
- [19] Jefferys, J. G. R. & Haas, H. L. (1982). Synchronized bursting of CA1 hippocampal pyramidal cells in the absence of synaptic transmission. *Nature*, 300, 448-450.
- [20] Viana, R. L., Borges, F. S., Iarosz, K. C., Batista, A. M., Lopes, S. R., Caldas, I. L. (2014). Dynamic range in a neuron network with electrical and chemical synapses. *Communications in Nonlinear Science and Numerical Simulation*, 19, 164-172.
- [21] Rulkov, N. F. (2001). Regularization of synchronized chaotic bursts. *Physical Review Letters*, 86, 183-186.
- [22] Hodgkin, A. L., & Huxley, A. F. (1952). A quantitative description of membrane current and its application to conduction and excitation in nerve. *The Journal of Physiology*, 117, 500-544.
- [23] Hindmarsh, L. J., & Rose, R. M. (1984). A model of neuronal bursting using three coupled first order differential equations. *Proceeding of the Royal Society of London Series B*, 221, 87-102.
- [24] Lapique, L. (1907). Recherches quantitatives sur l'excitation électrique des nerfs traitée comme une polarisation. *Journal de Physiologie et de Pathologie Générale*, 9, 620-635.
- [25] Brette, R. & Gerstner, W. (2005). Adaptive exponential integrate-and-fire model as an effective description of neuronal activity. *Journal of Neurophysiology*, 94, 3637-3642.
- [26] Touboul, J. & Brette, R. (2008). Dynamics and bifurcations of the adaptive exponential integrate-and-fire model. *Biological Cybernetics*, 99, 319-334.

- [27] Naud, R., Marcille, N., Clopath, C., Gerstner, G. (2008). Firing patterns in the adaptive exponential integrate-and-fire model. *Biological Cybernetics*, 99, 335-347.
- [28] Erdős, P. & Rényi, A. (1959). On random graphs, I. *Publicationes Mathematicae*, 6, 290-297.
- [29] Gelenbe, E., & Cramer, C. (1998). Oscillatory corticothalamic response to somatosensory input. *Biosystems*, 48, 67-75.
- [30] Semm, W., Wyler, K., Streit, J., Larkum, M., Lüscher H.-R., Mey, H., Müller, L., Stainhauser, D., Vogt, K., Wannier, Th. (1996). Dynamics of a random neural network with synaptic depression. *Neural Networks*, 9, 575-588.
- [31] Gabbiani, F. & Koch, C. (1998). Principles of spike train analysis, in *Methods in Neuronal Modeling: From Ions to Networks*, 2nd Edn, eds C. Koch and I. Segev (Cambridge, MA: MIT Press), 313-360.
- [32] Borges, R. R., Borges, F. S., Lameu, E. L., Batista, A. M., Iarosz, K. C., Caldas, I. L., Viana, R. L., Sanjuán (2016). Effects of the spike timing-dependent plasticity on the synchronisation in a random Hodgkin-Huxley neuronal network. *Communications in Nonlinear Science & Numerical Simulation*, 34, 12-22.
- [33] Kuramoto, Y. (2003). *Chemical oscillations, waves and turbulence*. Dover, New York.
- [34] Baptista, M. S., Zhou, C., Kurths, J. (2006). Information transmission in phase synchronous chaotic arrays. *Chinese Physics Letters*, 23, 560-563.
- [35] Zhang, W., Li, C., Huang, T., Xiao, M. (2015). Synchronization of neural networks with stochastic perturbation via aperiodically intermittent control. *Neural Networks*, 71, 105-111.
- [36] Lameu, E. L., Borges, F. S., Borges, R. R., Iarosz, K. C., Caldas, I. L., Batista, A. M., Viana, R. L., Kurths, J. (2016). Suppression of phase synchronisation in network based on cat's brains. *Chaos*, 26, 043107.

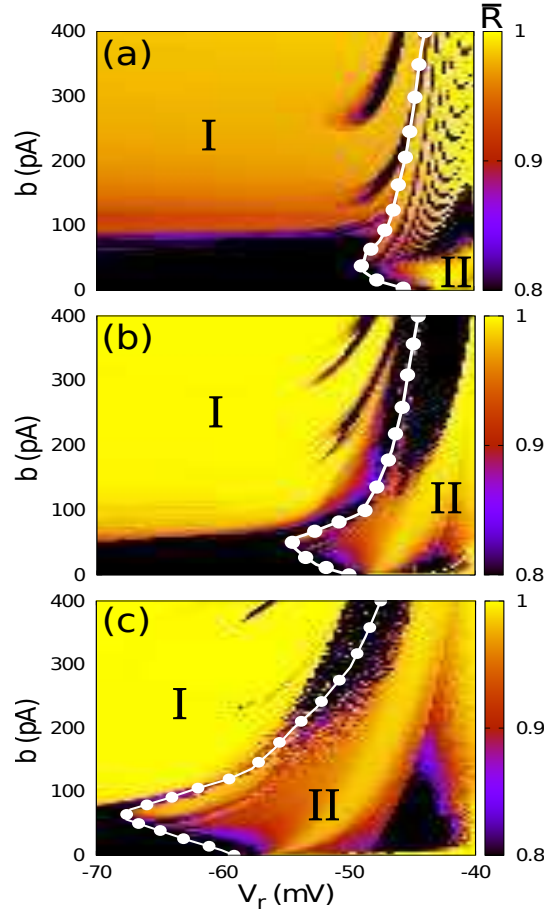


Figure 7: (Colour online) Parameter space  $b \times V_r$  for  $p = 0.5$ ,  $\gamma = 0$  (a)  $g_{\text{ex}} = 0.05\text{nS}$ , (b)  $g_{\text{ex}} = 0.25\text{nS}$ , and (c)  $g_{\text{ex}} = 0.5\text{nS}$ , where the colour bar represents the time-average order parameter. The regions I (spike patterns) and II (bursting patterns) are separated by white circles.

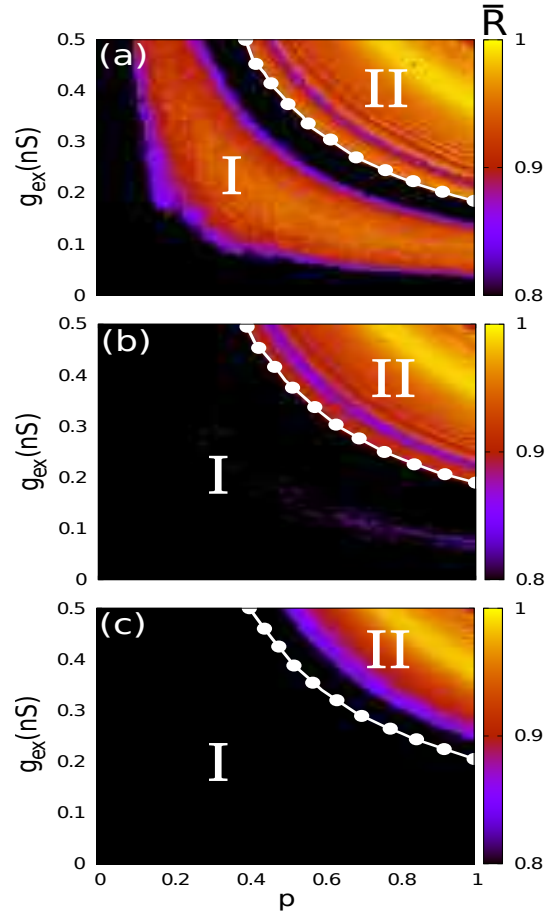


Figure 8: (Colour online)  $g_{\text{ex}} \times p$  for  $V_r = -58\text{mV}$ ,  $b = 70\text{pA}$ , (a)  $\gamma = 250\text{pA}$ , (b)  $\gamma = 500\text{pA}$ , and (c)  $\gamma = 1000\text{pA}$ .



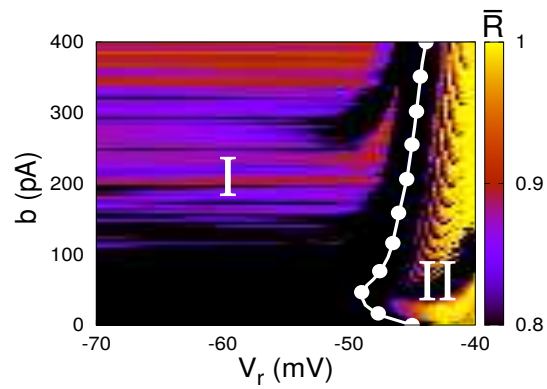


Figure 9: (Colour online)  $b \times V_r$  for  $g_{ex} = 0.05\text{nS}$ ,  $p = 0.5$ , and  $\gamma = 500\text{pA}$ , where the colour bar represents the time-average order parameter. The regions I (spike patterns) and II (bursting patterns) are separated by white line with circles.